Optical and Electronic Reflectivity of TaS_2

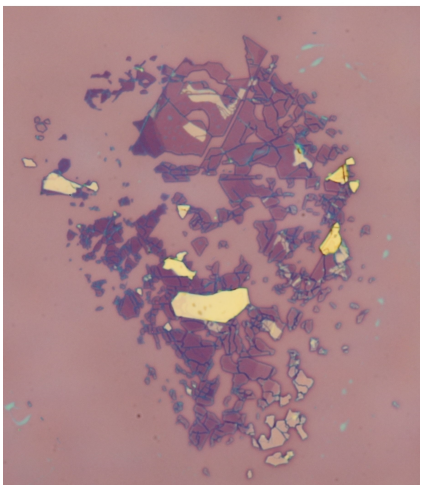

THESIS

submitted in partial fulfillment of the
requirements for the degree of

BACHELOR OF SCIENCE
in
PHYSICS

Author :	Jean-Paul van Soest
Student ID :	1650939
Supervisor :	Prof.dr.ir. Sense Jan van der Molen
	Tobias A. de Jong, MSc
2nd corrector :	Prof.dr. Jan M. van Ruitenbeek

Leiden, the Netherlands, June 29, 2018

Optical and Electronic Reflectivity of TaS_2

Jean-Paul van Soest

Huygens-Kamerlingh Onnes Laboratory, Leiden University
Niels Bohrweg 2, 2333 CA Leiden, the Netherlands

June 29, 2018

Abstract

When Van der Waals materials are reduced to two-dimensional atomic crystals, their physical properties start to change. For most materials these properties and phenomena are still unresearched. Van der Waals materials can be created to be atomically thin, to layers of a single atom thick. One class of these materials are transition metal dichalcogenide materials (TMDs). There exist different crystalline structures of TMDs, which are called polytypes. Here, TaS_2 flakes are fabricated in order to study charge density waves (CDWs). A protocol to fabricate large thin flakes is developed along with a simple and quick method to determine the layer thickness with the use of an optical microscope. The calculated thicknesses are then verified with Atomic Force Microscopy (AFM) measurements. Low Energy Electron Microscopy (LEEM) measurements are performed on thick flakes in order to research CDWs. Although confirmation of CWDs is absent, different domains of reflective electron intensity and various structures are observed. These features are compared with AFM measurements. The flake existing of different polytypes could be the cause for the observed contrasts. The reflection of electrons is observed until an energy of 150 eV.

Contents

Chapter 1

Introduction

1.1 Background

Dimensionality is one of the most influential material parameters. When three-dimensional atomic crystals get thinner and thinner, their physical properties start to change. Many of these properties and phenomena are for most materials still unknown. However, not all materials can be reduced to two dimensional sheets, only layered materials can.

The first discovered material to be reduced to a single layer was graphite (graphene for a single layer). Theorists have been writing about graphite being able to exist as a monolayer since 1947. [1] But only in 2004 Andre Geim and Konstantin Novoselov were able to fabricate and isolate graphene, for which they received the Nobel prize in 2010. [2] These single layers were made by a surprisingly simple new technique called exfoliation. Exfoliation is also called the Scotch tape method, since a certain tape is pressed on a atomic crystal and then removed while picking up thin layers of the material. In Chapter 3 exfoliation is explained more extensively. Since its discovery, graphene has been one of the leading topics in condensed matter physics.

By now, the scientific attention has expanded towards other isolated atomic planes, these are Van der Waals materials. These materials are built up from separate layers. The atoms within a layer are held together with strong covalent bonds, while different layers are only held together by weak Van der Waals interactions. This is the reason why exfoliation is possible.

One class of Van der Waals materials are transition metal dichalcogenide materials (TMDs). TMDs have a chemical formula of the form MX_2, where M is a transition metal (Mo, W, etc.) and X a chalcogen atom (Se, O, etc.). There is a whole family of TMDs, each with its own physical properties. TMDs are interesting, because in the two-dimensional limit they have small direct band gaps, making them compelling for possible future applications. Some examples of possible important applications are energy storage and conversion of sunlight into electricity with great efficiency. [3] In the next chapter TMDs are explained in greater detail.

One interesting TMD is TaS_2. In thin flakes TaS_2 has different crystalline phases. Different phenomena and properties appear with these different polytypes, like a different band structure. Another interesting feature of some TMDs are charge density waves (CDWs). CDWs occur when the spatial formation of atoms gets altered, resulting in a periodic density of charge. [4–6] These crystalline phases and CDWs are promising phenomena for future research.

1.2 Research

Nowadays there is a lot of research on two-dimensional TMDs. [3, 7–11] However, there are two major challenges. The first is the sample fabrication. This is done by exfoliation from a thick crystal as mentioned above. Although it is quiet common to make thin flakes, each research group has its own method. Some use liquid exfoliation, where the crystal is submerged in a solvent and thin flakes are deposited. [12] The disadvantages of liquid exfoliation are that working with liquids is always more tedious, since one always has to remove residues, and the deposited flakes are small. As mentioned before, another common technique is mechanical exfoliation. This way, thicker and thinner flakes stick to the tape. The problem is that there is a lot of local knowledge and it is hard to find literature as papers tend not to focus on the fabrication of samples. Exfoliation is also researched here and the best method to fabricate the largest and thinnest flakes is described in the Chapter 3.

The second challenge is that the process to determine the layer thickness is quite cumbersome. This is usually done with techniques such as Atomic Force Microscopy (AFM) and Raman spectroscopy, since these techniques are reliable. [13, 14] However, these processes ask for additional equipment and are very time-consuming, especially if one has large flakes and many samples. Therefore, a simple method to determine the thickness of TMDs is highly desirable. For a few TMDs, such as MoS_2, there exists a simpler method using an optical microscope. However, this is only applicable to these specific TMDs, because each TMD has its own properties, such as absorption efficiency of light and refractive index. In this thesis a developed method is described, which uses an optical microscope to determine the optical contrast of TaS_2 flakes with different thicknesses with the substrate. These contrast values can be used to calculate the thickness of flakes. Optical photos can be taken directly after stamping, which makes the process a lot quicker. The thicknesses were then verified with AFM measurements. The method is described in Chapter 3.

After the sample preparation, the optical contrast determination and the thickness verification, the flakes were measured with Low Energy Electron Microscopy (LEEM). This technique uses electrons instead of photons as with optical microscopy, which provides certain advantages. For example, different polytypes could be distinguished. This, and other properties, are described in Chapter 3. The hypothesis stated that these flakes would be of a single polytype and would appear to be uniform. However, with these measurements much more structures and domains were seen than expected. These properties will be described and are studied here.

Chapter 2

Theory

2.1 Transition metal dichalcogenides

There are more than forty members in the family of TMDs. [15] In theory, every combination of a transition metal and a chalcogen is possible. TMDs have a molecule formula of the form MX_2. Transition metals can be found in the middle of the periodic table, ranging from part of group 3 to group 10. Chalcogen atoms are all the elements in group 16. However, almost all currently known TMDs are build from the elements as seen in Figure 2.1.

TMDs are compound of different polytypes, this is the orientation of atoms within separate layers with respect to each other. Different polytypes have different unit cells, of which the layers are built up. The simplest polytype is 1T. 1T-layers can be stacked in two different ways. These vary in whether the two adjacent chalcogen atoms lie above or shifted from each other. These variations are called respectively 1T and 1T'. Other frequently occurring polytypes are 2H, 3R, 4H and 6R, these can be seen in Figure 2.2. The number represents the number of layers a unit cell consists of. The letter represents the structure of the crystal lattice: T stands for trigonal, H for hexagonal and R for rhombohedral, as can be seen in Figure 2.3a). The main difference within a single layer is the orientation of the chalcogen atoms with respect to each other. In the 1T-case the chalcogen atoms of a single atom lie 60° shifted, while in the 2H-case these lie directly above each other. Some polytypes also have different varieties, such as the 4H-polytype (a, b, c, d_I and d_{II}). A TMD can be build up from all combinations of these unit cells, creating a certain stacking sequence. This forms different domains within a single crystal.

The TMD researched in this thesis is TaS_2. This material is relatively unresearched, however nonetheless fascinating. The band structure of TaS_2 has a direct band gap, but for the different polytypes the band structure differs. This can be seen in Figure 2.3b) for 1T and 2H. Because of this, electrons can be absorbed by the material at different energies. This provides a contrast between 1T- and 2H-domains in LEEM measurements.

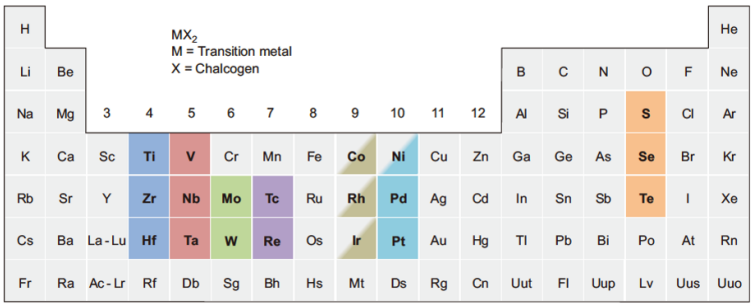

Figure 2.1: *The periodic table with the most common transition metals and chalcogens of TMDs highlighted. Taken from [15]*

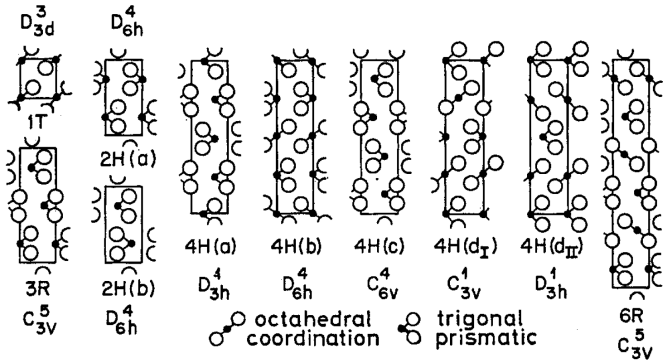

Figure 2.2: *Side view of the most common crystalline phases of TaS_2 and their variations. Taken from [4]*

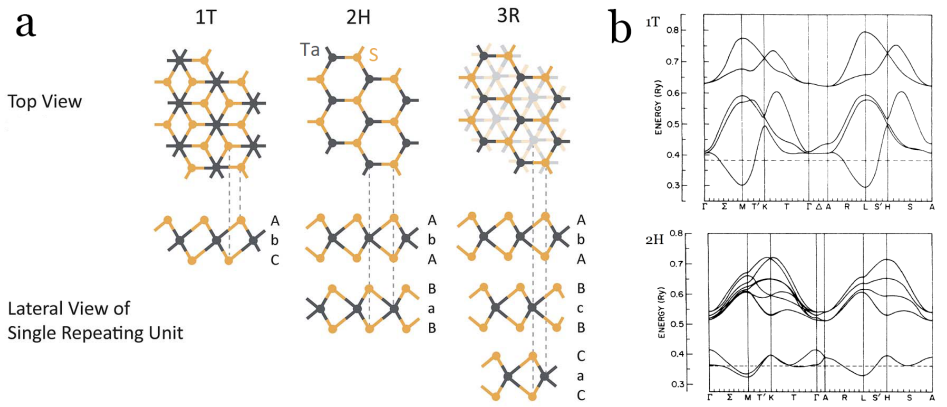

Figure 2.3: (**a**) *Top and side view of three crystalline phases, 1T, 2H and 3R, of TaS_2. In the top view the trigonal, hexagonal and rhombohedral structure of the lattice can be seen. Adapted from [10]* (**b**) *Calculated band structures of 1T- and 2H-TaS_2. Adapted from [16]*

Another difference between the 1T- and the 2H-polytype is the lattice constant of the crystal lattice. These values follow from a simple derivation (adapted from [17]). The system can be treated as nearly free electrons in a periodic potential. This gives rise to the dispersion relation, the relation between the energy and the momentum of the electrons:

$$E_k = \frac{\hbar^2 |\mathbf{k}|^2}{2m_e} \qquad |\mathbf{k}| = \frac{2\pi}{\lambda} \tag{2.1}$$

where $\mathbf{k}$ is the wave vector, which can be written in terms of the wave length λ, and m_e is the effective electron mass. The wave vector can either be expressed in the lattice vectors $\mathbf{a}$, $\mathbf{b}$ or the reciprocal lattice vectors $\mathbf{a}^*$, $\mathbf{b}^*$:

$$\mathbf{k} = l\mathbf{a}^* + m\mathbf{b}^* = \mathbf{G}_{lm} \tag{2.2}$$

$$\mathbf{a}^* = 2\pi \frac{\mathbf{b} \times \hat{\mathbf{n}}}{|\mathbf{a} \times \mathbf{b}|} \qquad \mathbf{b}^* = 2\pi \frac{\mathbf{a} \times \hat{\mathbf{n}}}{|\mathbf{b} \times \mathbf{a}|} \tag{2.3}$$

Here $\mathbf{G}_{lm}$ is a reciprocal lattice vector. For a hexagonal grid the lattice constant a is related to the lattice vector as follows: $a = |\mathbf{a}| = |\mathbf{b}|$. In Low Energy Electron Diffraction (LEED) measurements at low energies only the zeroth order diffraction spot can be seen. When increasing the energy, the first order spots appear at an energy corresponding to a momentum equal to the reciprocal lattice vector of the appearing first order diffraction spots. This can be expressed with inequation 2.4:

$$|\mathbf{G}_{lm}| \leq \frac{\sqrt{2m_e E_k}}{\hbar} \tag{2.4}$$

With these equations the lattice constant a can be calculated. With a hexagonal grid and first order diffraction spots, this becomes:

$$|\mathbf{G}_{01}| = \frac{2\pi}{a \sin\left(\frac{1}{3}\pi\right)} \tag{2.5}$$

$$a = \frac{4\pi}{\sqrt{6}} \frac{\hbar}{\sqrt{m_e E_{01}}} \tag{2.6}$$

The lattice constant found in this research is shown in the Chapter 4.

2.2 Optics

When TaS_2 on a substrate of silicon or silicon dioxide is placed under an optical reflection microscope, different thicknesses appear in different intensities, sometimes even different colours. This is even the case for thin

flakes. A single layered flake has a thickness of one lattice constant, which is a few Å thick. [16] Flakes are still considered to be thin when the are a few dozens of layers thick. The wavelength of optical light is between 390 and 700 nanometer. Because of this, the pathlength difference of light reflected on the lower surface and on the upper surface of the flake is almost completely negligible. The effect of interference of light with a phase difference obtained from the path length difference within the flake does not, in itself, contribute in the contrast between different thicknesses. This applies as long as one looks at thin flakes.

In the case of silicon dioxide, the substrate consists of 300 nm of silicon dioxide on top of silicon that is a thousand times thicker. The silicon can thus be seen as infinitely thick. When there is a flake there are three different interfaces: air-TaS_2, TaS_2-silicon dioxide and silicon dioxide-silicon. At every interface a part of the light is reflected and a part is transmitted. The silicon dioxide layer (dielectric layer) acts as a Fabry-Pérot interferometer. Within this interferometer, when light comes in from the upper surface it gets partly transmitted to the silicon, where it is lost; and partly reflected, where it can again partly reflect at the upper surface. The light that travels up and down interferes with itself.

When there is no flake on the substrate, there is a well defined thickness of the interferometer and the reflected intensity and wavelength can be calculated. This interference results in the intensity and colour of the substrate. When there is a flake on top, the interferometer gets a bit larger and thus amplifies a different wavelength. This is the reason why flakes of different thicknesses have different colours. However, there are some other factors to take into account. The first is that TaS_2 has a different refractive index than the dielectric layer. This results in a slightly altered net refractive index of the interferometer. The second is that when light travels from a medium with a lower refractive index to a medium with a greater refractive index, there is a phase change.

Figure 2.4 shows the optical paths of light reaching the surface of a sample. On the left side the light directly reaches the substrate, on the right side there lies a thin flake on the substrate. Properties of the materials are also shown, like the thicknesses and refractive indices of the materials (d_j and n_j, where the index $j = 1, 2, 3, 4$ representing air, TaS_2, silicon dioxide and silicon respectively).

The reflection intensity of the reflected light can be calculated (adapted from [18]). When there is no flake, the light gets partly reflected on and partly transmitted through the dielectric material. This results in a phase

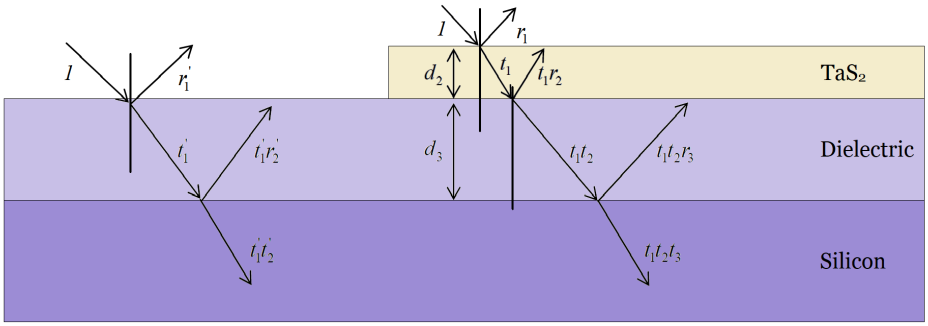

Figure 2.4: *Optical reflection and transmission for a silicon dioxide substrate (left) and a flake on silicon dioxide (right). Several optical paths are shown with at each intersection a reflection and a transmission. Adapted from [18]*

change δ_3' and reflected amplitude r'_{total}*:

$$\delta_3' = \frac{2\pi}{\lambda} d_3(n_3 - ik_3) \tag{2.7}$$

$$r'_{total} = \frac{r_1' + r_3' e^{-2i\delta_3'}}{1 + r_1' r_3' e^{-2i\delta_3'}} \tag{2.8}$$

where $i^2 = -1$ and k_j is the imaginary part of the complex refractive index, also known as the extinction coefficient. The prime represents the case when there is no flake.

When there lies a flake on the substrate this gets slightly more complicated, since there is now an extra layer with its own thickness and refractive index to take into account. The phase changes due to the flake and the dielectric material are now respectively:

$$\delta_2 = \frac{2\pi}{\lambda} d_2(n_2 - ik_2) \tag{2.9}$$

$$\delta_3 = \frac{2\pi}{\lambda} d_3(n_3 - ik_3) \tag{2.10}$$

*Here r_1' is the reflection amplitude between air and silicon dioxide and r_2' is the reflection amplitude between silicon dioxide and silicon.

The total reflected light now depends on the thickness and the (complex) refractive index of all three materials. The total reflected amplitude can be written as[†]:

$$r_{total} = \frac{r_1 + r_2 e^{-2i\delta_2} + r_3[r_1 r_2 + e^{-2i\delta_2}]e^{-2i\delta_3}}{1 + r_1 r_2 e^{-2i\delta_2} + r_3[r_2 + r_1 e^{-2i\delta_2}]e^{-2i\delta_3}} \tag{2.11}$$

To now get the reflected intensities the (complex) reflection amplitude is squared:

$$R_{substrate} = r'_{total} r'^{*}_{total} \tag{2.12}$$

$$R_{flake} = r_{total} r^{*}_{total} \tag{2.13}$$

The contrast between the flake and the substrate is thus given by:

$$contrast = \frac{R_{flake} - R_{substrate}}{R_{flake} + R_{substrate}} \tag{2.14}$$

In this thesis flakes are researched on two different substrates: silicon and silicon dioxide. The calculations above are for silicon dioxide, but greatly simplify for the silicon substrate. This is because there is now only a dielectric layer, and thus a Fabry-Pérot interferometer, of 10 nm. When d_3 gets this small, δ_3 gets small and equations 2.8 and 2.11 can be approximated with:

$$r'_{total} = \frac{1}{r'_1} \qquad\qquad r_{total} = \frac{r_1 r_2 + e^{-2i\delta_2}}{r_2 + r_1 e^{-2i\delta_2}} \tag{2.15}$$

The intensity difference between thicker and thinner flakes is now solely caused by the absorption of light by the layers of TaS_2. On a substrate of silicon all flakes are thus expected to have the same colour; different thicknesses only reflect a different intensity. This is because when d_2 differs from small to large, δ_2 differs accordingly and, as can be seen in equations 2.15 and 2.13, the reflection amplitude R_{flake} also differs accordingly. Therefore, only the intensity varies between thick and thin flakes.

[†]Here r_1 is the reflection amplitude between air and TaS_2, r_2 the reflection amplitude between TaS_2 and silicon dioxide, and r_3 the reflection amplitude between silicon dioxide and silicon. To see how r_1, r_2 and r_3 are calculated, see [18]

2.3 Charge density waves

CDWs occur when the spatial formation of atoms gets altered. When certain atoms in a crystal lattice come to stand closer to each other and certain atoms further away, a periodic density of charge is created, as can be seen in Figure 2.5. A CDW-transition is a consequence of the strong electron-lattice coupling in the lattice. [19] In order for a CDW-transition to occur, a large and stable anisotropy must be present within the crystal lattice. The rearrangement of the atoms results in an enhanced electron-phonon interaction. The electrons within a CDW can flow with much less resistance through a material.

TMDs are constructed of layers with strong covalent bonds and exist in different polytypes. TMDs are thus a class of materials where CDW-transitions can occur, since there exist different arrangements of the atoms within the layers. TaS_2 has a CDW-transition above room temperature, which eases scientific research. CDWs are expected to be observed especially in the 1T-polytype of TaS_2, because its Fermi surface is relatively simple with large near-parallel walls, which favours CDWs. [4]

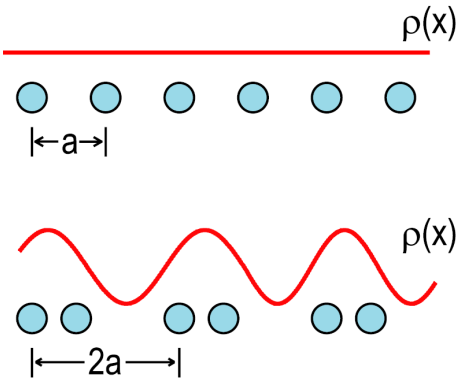

Figure 2.5: *A monatomic linear chain of atoms before (top) and after (bottom) a CDW-transition. The positions of the atoms are shifted, which results in a periodic charge density (CDW). Taken from [19]*

Chapter 3

Experimental techniques & Methodology

3.1 Sample fabrication & exfoliation

3.1.1 Fabrication

As explained in the Chapter 2, exfoliation can be performed on TMDs. We started with a crystal of TaS_2 commercially bought from HQ graphene. [20] The crystal is grown in the 1T-structure and is approximately 10 mm in diameter.

Two different substrates are used: silicon with a 300 nm thick layer of silicon dioxide and silicon. The former has the advantage that flakes of TaS_2 are clearly visible with an optical microscope. Different thicknesses appear in different colours. The hypothesis stated that the colour corresponds with a certain thickness: starting from really thick down to single layers the colours go from yellow to blue to purple. Many TMDs, such as MoS_2 and WSe_2, have a light colour when they are more than ten layers thick. They only obtain a dark colour at three or four layers thick or thinner. [21] A similar behaviour was expected for TaS_2. For thin flakes the assumption is taken that the colour of the flake depends linearly on the thickness. The major disadvantage of this substrate is that it is not a conductor. Therefore, in order to do LEEM measurements, for which conductivity is necessary, conducting leads should be made on the flake. This is however an extra unwanted step. Therefore, a second substrate was used: doped silicon. This is a semiconductor and can thus be used for LEEM measurements. The surface of this substrate only has a 10 nm of silicon dioxide layer. The disadvantage of this substrate is that the flakes are a lot less visible with optical microscopy, of which the reason is described in Chapter 2. Also, every thickness has the same colour, only a different intensity. This makes it harder to identify the layer thicknesses of the flakes. Both substrates are used for this thesis, however only samples on a substrate of silicon are used for LEEM measurements.

The sample fabrication is completely done in the cleanroom facility in Leiden. The first thing to do is the cleaning of the substrate, since it has always

assembled a lot of dirt from being in open air. The substrate is sonicated: firstly in water, secondly in acetone and thirdly in isopropanol (IPA), all for five to ten minutes at 45 °C. Ethanol and acetone are used to remove dirt particles and organic particles. When exposed to air after the acetone treatment, it always leaves a residue. The IPA treatment prevents this residue to form, when applied immediately after the acetone. After the sonicating the substrate is blown dry with nitrogen.

The second part of the cleaning procedure is placing the substrate in the ozone cleaner. In here the substrate is submitted to an ozone flow for more than fifteen minutes. Most organic particles still present on the substrate are now removed. There is also still oxidation on the substrate. When the oxydised substrate is treated with ozone, a chemical reaction occurs where only O_2, CO_2 and H_2O are formed.

During the ozone cleaning, the exfoliation is performed. A clean strip of tape is gently placed on the grown crystal. It is pressed with a cotton bud in order to get as much flakes as possible. The tape is then gently pulled of the crystal. A thin layer of TaS_2 has come off and is now sticking to the tape. This thin layer is however still hundreds of layers thick. To reduce the thickness another tape is placed on the first tape and another exfoliation is performed. This process is repeated a number of times, usually from three to ten times.

When the ozone cleaning is done, it is time for the stamping. This is done as quickly as possible, within a few minutes, in order to prevent new pollution from the air. The process of stamping is similar to exfoliation. The substrate is put down on a clean surface. The final tape used, is now placed on the substrate and again is pressed down with a cotton bud, now in order to leave as many flakes behind as possible. The tape is gently pulled off of the substrate and now we can, even by eye, see flakes on the surface.

The substrates are not cleaned again after stamping. Although there is also glue transferred from the tape to the substrate, this is only a little. With cleaning one would also wash off a large part of the flakes of the substrate.

3.1.2 Optimising exfoliation & stamping

Every research group seems to have its own method on how to get the largest and thinnest flakes. [3, 7–12, 22] Therefore, some parameters were tested here. The substrate is already cleaned, so we focused on the exfoliation and stamping. By far the most influential parameter on the result of the sample fabrication is the number of tapes used. The hypothesis stated that the more tapes you use, the thinner the flakes become, because each time

you tear the tape loose it takes along a few layers from the thicker flake you started with. The more tapes you use, the more times a few layers a taken along and the flake gets thinner and thinner.

Another parameter tested is heating. [11, 22] During stamping one can heat the substrate. The hypothesis stated that heating results in more flakes getting released from the tape and remain on the substrate. Both temperature and heating time were varied. The results of both the number of tapes used and the heating are discussed in Section 4.1.

3.2 Optical microscopy

To determine the layer thickness of TaS_2 flakes, optical microscopy is used. The first optical microscope used takes black-and-white photos and is placed in the cleanroom in Leiden. One big advantage is that one can take images directly after fabricating the sample, because this is also done in the cleanroom. Reflection microscopy with a white light source is used. The magnification ranges from 5x to 100x. In order to ease the layer thickness determination later on, different optical filters were used. Of every flake photos were taken without a filter (white light), with a blue band-pass filter ($\lambda = 500 \pm 12$ nm) and with a red high-pass filter ($\lambda \geq 720$ nm). In Figure 3.1 the effect of these filters is shown. By using these optical filters, different thicknesses of flakes have different intensities on the photos. This makes it is possible to combine the contrasts found in the set of photos in order to get more accurate results.

The use of colour filters improves the thickness determination, however this is not optimal. Therefore a second microscope is used, one that takes colour photos. All properties mentioned above are the same for this microscope. Taking photos through this microscope greatly eases the thickness calculations.

Also, a standardised method to take the microscopy photos is created. In order to determine the thickness of flakes, photos have to be taken with standard parameters. With an exposure time of 3 ms and a consequent light intensity (at the microscope in the cleanroom in Leiden at setting 8). This results in the same colours, contrasts and intensities of flakes and enables the photos to be analysed.

3.3 Optical image analysis

A Python program LayerThicknessCalculator is written to easily analyse the optical microscopy photos. The user can draw a segmented line over

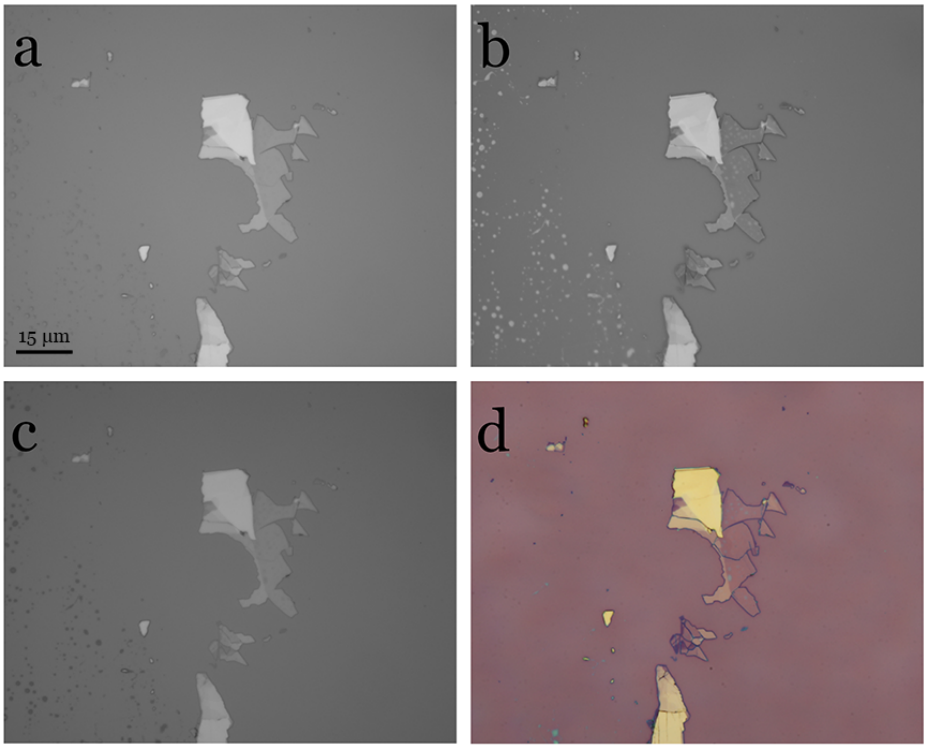

Figure 3.1: *Exfoliated TaS_2 on silicon dioxide.* (**a**, **b**, **c**) *Respectively taken with no, a blue and a red colour filter in Leiden.* (**d**) *Taken with the colour camera through the second microscope used.*

each area of a flake and one part on the substrate. Then, the intensity of every pixel on the line is calculated and normalised. A clustering algorithm (KMeans) finds different areas, which all have a different thickness. Now the ratio of optical contrasts are calculated by comparing each area with each other.

Since the flakes are also measured with AFM, as described in the next section, the ratio found can be compared with the thicknesses of the flake.

3.4 Atomic Force Microscopy

3.4.1 Setup

Atomic Force Microscopy (AFM) is an imaging technique developed in the early eighties. [23] The height of a surface is measured, this is either done by touching the surface with a probe, or by coming really close to it. The probe is a few-micrometer long tip, attached to a flexible cantilever. A laser

is reflected on the cantilever. When a force acts on the tip, the cantilever bends and the reflection of the laser on the photodiode is displaced. From this displacement the height of the surface is calculated. The tip moves back and forth over the sample, measuring line by line. The height of the tip is continuously adjusted by a feedback loop, controlling the piezo motors of the three legs of the AFM. The result is an image, a height map, of the sample. Besides the height, also other parameters are measured, such as the error signal, the lock-in amplitude, the lock-in phase etc. For all these channels data from the trace and retrace are obtained.

The most common measuring technique is tapping mode (also called dynamic contact or AC mode). Here, the tip is oscillating close to the resonance frequency. When the tip gets close to the surface, it feels the attractive or repulsive Van der Waals force between the atoms of the tip and the atoms of the sample. When the tip and the sample are far away from each other, there is, in general, an attractive force (when the sample is not charged). When they are really close to each other, there is a steep repulsive force. This phenomenon is clearly seen in the Lennard-Jones potential (also called London dispersion or Van der Waals forces), as shown in Figure 3.2b). The force alters the amplitude and phase of the oscillation of the tip, which are also measured. An advantage of tapping mode is that the tip is for most of the time not in contact with the sample. Therefore, the lateral forces are much smaller than with contact mode and the chance to damage the sample is much less. However, the perpendicular force on the sample is greater.

Another measuring technique is Quantitative Imaging (QI) mode. In this mode, the tip is also in intermittent contact with the surface. Here, the tip is not oscillating, but instead slowly approaching the surface. When the tip is in contact with the sample, it is pressed until a predetermined force is reached. Then the tip releases pressure and rises again. This is done separately for every pixel of the image. The perpendicular force with QI mode is greater than with tapping mode, however there are almost no lateral forces.

No matter which imaging mode is used, there are always artifacts, of which two major causes are the shape and the velocity of the tip. A sharp tip gives the most realistic image. The reason for this is, when approaching, for example, an upstanding edge, always the side of the tip touches the edge first. This causes the tip to rise and thus measuring a height increasement before the point of the tip reaches the edge. This results in a ramp to be imaged instead of a vertical edge. The same goes for edges downwards. Also, there are areas just behind edges that the tip can not reach, so that a "shadow", a height shifted up- or downwards, is imaged. This issue is resolved by measuring a trace and a retrace. When the measurement is done in the other

direction, it is possible to measure the surface within this "shadow". For QI mode, because here the tip approaches the sample perpendicularly, the measured height of every pixel is independent. This results in less artifacts than tapping mode.

3.4.2 Measurements

AFM measurements are necessary, because with optical microscopy only the optical contrast can be calculated and it only gives the correct ratios. This is because you do not beforehand know whether the thinnest part of the flake is a single layer. AFM measurements can give a decisive answer. For most of this research tapping mode was used, since the flakes should not be damaged. Some flakes were also measured with QI mode in order to confirm the results and to get more accurate results. The AFM used is manufactured by JPK and is shown in Figure 3.2a). The cantilever uses has a resonance frequency of 70 kHz and a spring constant of 5 N/m. In order to get the highest quality images, parameters such as the setpoint amplitude, driving frequency, gain, frequency of the tip in the fast imaging direction and the number op pixels in the image are optimised. There is however a problem when measuring two different materials, which is exactly what is done in this research, because we want to know the thickness of flakes on a substrate. All materials have a different Lennard-Jones potential, as shown in Figure 3.2b). When a tip approaches surfaces of two different materials, it thus feels a different force. This results in a different height measured, even when two materials are equally thick. Thus, instead of the true height, an apparent height is measured. [24] The apparent height is an indispensable artifact. However, this artifact can be reduced by choosing the measuring parameters such, that the forces felt during the measurements are approximately equal. Besides this Lennard-Jones potential, also other unwanted forces influence the cantilever.

The flakes of TaS_2 were first found by an optical microscope. An average flake is larger than the measurable area when aligned, which is $30 \times 30\mu$m. An appropriate area on the flake to measure should be picked. It is recommended to have the direction of the tip movement perpendicular to an edge to get the clearest image. With this, the tip always approaches an edge from the same direction and a hard boundary is imaged. However, a second measurement can also be performed which is 90° rotated.

3.4.3 Data analysis

When an AFM measurement is done, the data are not always clear and artifacts can disturb the image. In order to analyse the data, these need to be resolved. For the data processing a program called Gwyddion [25] is used.

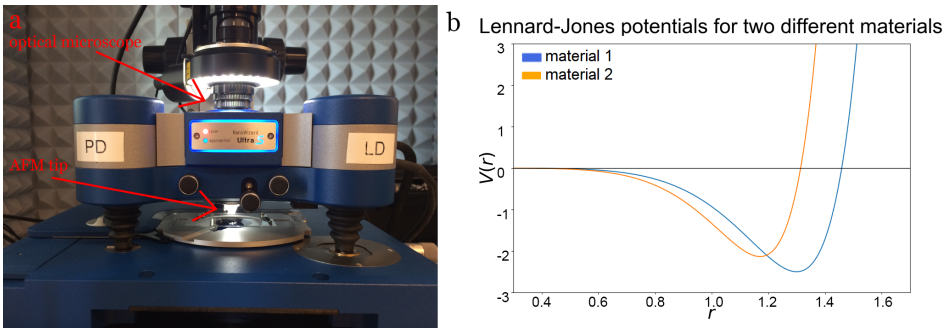

Figure 3.2: (**a**) *Photo of the AFM. On top is the optical microscope. At the bottom is the tip.* (**b**) *Lennard-Jones potentials of two different materials.*

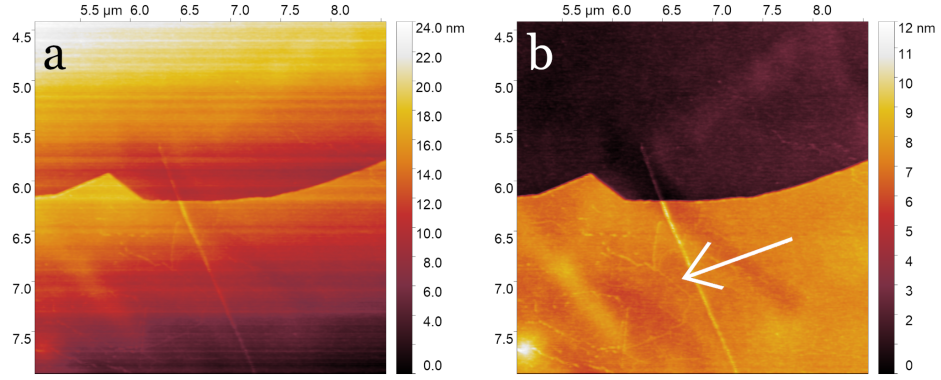

Figure 3.3: *AFM image of a region on a flake of TaS_2. The two clear distinguishable areas are caused by a thickness difference.* (**a**) *Raw data.* (**b**) *Processed, here new structures can be distinguished, as denoted by the arrow.*

This program can remove most artifacts of the image. Before processing an image looks like Figure 3.3a). A couple of procedures are applied to process the data. Firstly, the path leveling tool is used. Here a number of lines on the image is selected. The height values on these lines are then used for leveling. All rows on the line are adjusted up or down in order to minimize the height difference of the points. Secondly, the facet level tool is used. This levels the data by recognising facets and subtracting a plane from each of these facets. This results in horizontal areas, which are, for example, layers of a flake. Lastly, the colour range of the image is adjusted. Here a range from the lowest to the highest value of the height are selected, in order to get the greatest contrasts. The end result can be seen in Figure 3.3b). Now different structures can be distinguished, for example as denoted by the arrow.

In the next chapter the AFM measurements will be compared with the optical microscopy photos and the LEEM measurements.

3.5 Low Energy Electron Microscopy

Low Energy Electron Microscopy (LEEM) differs from optical microscopy in that it uses electrons instead of photons. With optical microscopy one can use visible light, infrared or ultraviolet spectra. IR and UV light often reveal various phenomena that can not be seen with visible light. By varying the wavelength, the energy also changes. There is however one major disadvantage to optical microscopy: the diffraction limit, which restricts the maximal resolution, see equation 3.1.

$$\Delta x = 1.220 \, \frac{f\lambda}{D} \tag{3.1}$$

where Δx is the spatial resolution, f the focal length of the objective, λ the wavelength and D the diameter of the lens' aperture.

$$p = \sqrt{\frac{E^2}{c^2} - m^2c^2} \tag{3.2}$$

$$\lambda = \frac{h}{p} \tag{3.3}$$

where h is the Planck constant, p the momentum of the photon, E its energy and c the speed of light. Equation 3.1 states that no greater resolution can be reached smaller than half the wavelength of the photons. Two point sources can be distinguished when the maximum of the first coincides with the first minimum of the second. With visible light an optimal resolution can be reached where structures of a few hundred nanometers can be imaged, while interesting structures of TMDs are only a few nanometers large.

This problem can be avoided by using electrons instead of photons. This is because electrons have a much smaller wavelength, given by the de Broglie equation (equation 3.3), of a few tenths or hundredths of nanometers. Thus much smaller structures can be imaged with electrons, than with photons. The same as in optical microscopy where one can use light with different energy spectra, here the energy can be varied in order to see different phenomena.

LEEM is a technique that uses the reflection of electrons with an energy range from 0 to 150 eV. The microscope used in this research is the ESCHER

LEEM. It is an aberration correcting LEEM, built by SPECS GmbH, following the design of Ruud Tromp. [26, 27] The low energies used give the opportunity to use electron microscopy on the samples without destroying them. Another advantage is that these energies correspond with many material properties, such as electronic transitions and electronic bands and band gaps.

Figure 3.4 shows the schematic setup of the LEEM. The electron source is an electron gun, which fires electrons with an energy of -15 keV. After going through some lenses and deflectors, the electrons reach the first magnetic prism. This prism produces a magnetic field, such that the electrons are deflected 90°. There they reach the sample, where the electrons are absorbed or reflected. The sample is put on a voltage of $+15$ keV $-\delta E_{landing}$, which decreases the velocity of the electrons. The voltage of the sample can be adjusted with an energy $E_{landing}$ of the order of single eV, causing the electrons to have a landing energy of a few eV when reaching the sample. A part of the electrons is reflected by the sample and accelerate back towards the magnetic prism. This also happens with secondary electrons that leave the sample. At the prism they get again deflected 90°, towards a second prism. Here is the second arm of the LEEM and adjusts the path of the electrons in order to correct for aberrations that were induced in the pathway before. This is done with an electron mirror. When the electrons come back to the second prism they are deflected towards the imaging system. The LEEM has an optimal resolution of 1.4 nm.

The imaging system consists of microchannel plates, to amplify the number of electrons; a phosphor screen, that converts electrons to photons; and a CCD, which detects the photons to make an image. These components however introduce consistent errors such as a dark count and a flat field. There is also always an error induced by the thermal drifting of the sample. Dark count is a thermally generated process which excites pixels, even when there is no light. This is countered by taking an image in complete darkness and subtracting this image from the measurements. Flat field is caused by the fact that each pixel has a different gain. This is resolved by first taking a flat field image. This is done in mirror mode (putting the voltage of the sample so, that all electrons are reflected before they reach the sample), which gives a maximum intensity. This flat field image is subtracted from the measurements. After the flat field correction a uniform input signal gives a uniform output signal. Drift correction is resolved by choosing a region of interest (ROI), which has distinct structures. A Python program compares this ROI with each image and finds different functions (polynomials) how the image is drifting in the x- and y-direction. One of these polynomials is chosen and all images are corrected accordingly.

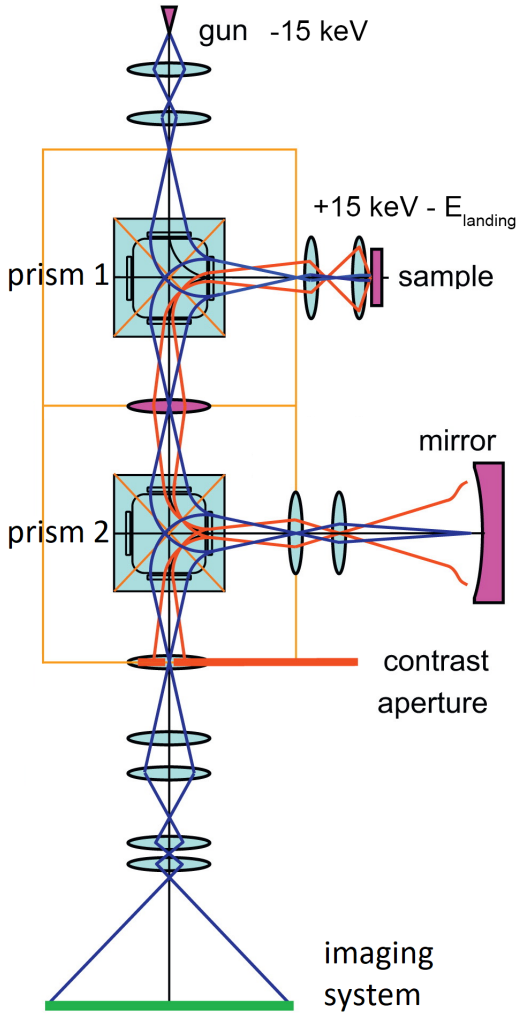

Figure 3.4: *Schematic setup of the LEEM. Adapted from [26]*

3.5.1 Measuring techniques

The LEEM provides different measurement techniques. Before measuring with LEEM, the first technique used is usually PhotoEmission Electron Microscopy (PEEM). With PEEM not electrons, but photons from an UV lamp are fired at the sample. The photons are absorbed by the sample, after which photo-electrons get excited and leave the sample. The smallest magnification is used to have the largest field of view. This is used in order to find the area of the sample one wants to measure on. A typical PEEM image is show in Figure 3.5a).

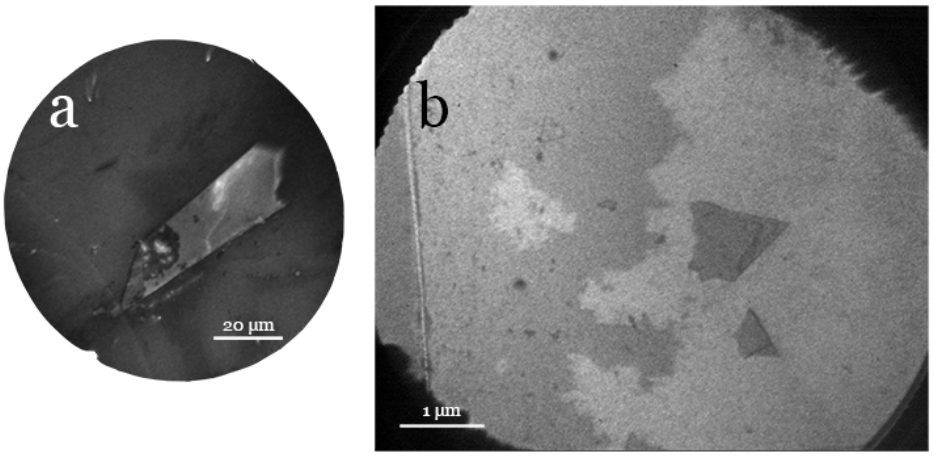

Figure 3.5: (**a**) *A typical PEEM image of a TaS_2 flake on silicon.* (**b**) *A typical Bright Field image of a part of a TaS_2 flake.*

A standard imaging technique is Bright Field imaging. When electrons are beamed to the sample, they are either reflected or absorbed. This results in a contrast in the intensity imaged. When the electrons have a high landing energy, also inelastic scattering occurs. This results in a spread in the energy and momentum of the reflected electrons. Secondary electrons leave the sample and are also imaged. The secondary electrons cause a background, or haze, over the image and thereby decrease in resolution. To increase the contrast, one can slide in an aperture that blocks part of the secondary electrons in reciprocal space and lets through mainly the electrons coming from elastic scatterings. These are the electrons from the zeroth order diffraction spot. This technique is called Bright Field imaging, as seen in Figure 3.5b).

Bright Field imaging is also used to make a series of images: an IV measurement. IV-LEEM is one of the most used measuring techniques, where I stands for the measured intensity of the reflection and V for the voltage or landing energy. With this technique the energy is slowly increased from mirror mode to a desired value. This generates a stack of images. Different ROIs can be chosen of which IV curves are plotted. The intensity is high when more electrons are reflected and low when more are absorbed. Whether an electron is reflected or absorbed depends on the electronic band structure of the material and on the energy of the beam. An electron gets absorbed if there is an electronic state in the material for its energy and momentum. When the beam is not perpendicular to the sample also the in-plane momentum needs to match the available state.
Besides Bright Field measurements, also the diffraction space can be imaged. The diffraction plane is the backfocal plane. In the focal plane, electron rays originating from the same point on the sample are focused on the

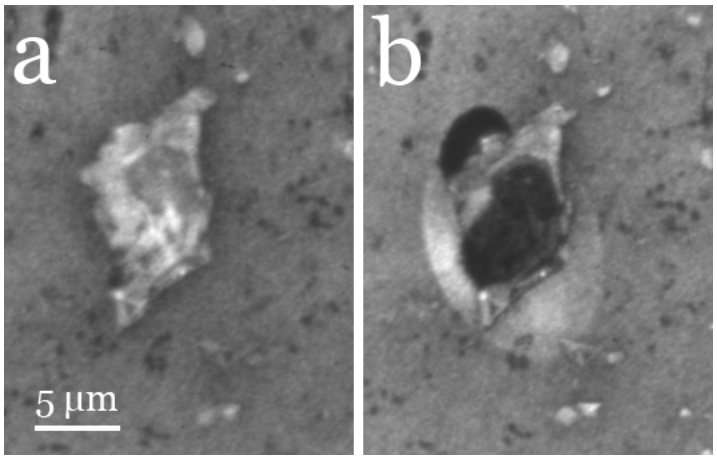

Figure 3.6: *PEEM images before* (**a**) *and after* (**b**) *the IV measurements. The clear dark ellipses in the flake are the imprints of the gun spot.*

same point. In the backfocal plane electron rays with the same angle originating from the sample are focused on the same point. The diffraction plane can thus be used to measure the angles of the electrons and also the angle, or tilting, of the sample. The imaging of the backfocal plane is called Low Energy Electron Diffraction (LEED). The electron beam reflects in different angles on different parts of the unit cell. By sliding in a second aperture, one can reduce the size of the illuminated spot on the sample and thereby focusing on very local areas of the sample. This technique is called μLEED. Another property of the material that could be extracted from μLEED measurements is the lattice constant. The calculation of the lattice constant can be found in Chapter 2. The energy used is the energy when the first order diffraction spots appear.

3.5.2 Method

Although the layer thickness determination with optical microscopy used thin flakes, for LEEM measurements it was decided to use thick flakes, of a few hundred layers thick. These thick flakes were easy to recognise since they were almost completely yellow in optical microscopy. Other criteria for measurement-flakes were that they were large enough (at least a few tens of micrometers in diameter), they had to be in one piece (some flakes were torn apart) and they needed to be clean (no dirt, glue or many small flakes lying on top). When good flakes were found, overview photos were taken with ”landmarks” that could easily be found with the LEEM. In order to find the region of interest more quickly, one could use markers (for example, by scratching arrows in the substrate). When the sample was mounted in the LEEM, the flakes were found by searching with PEEM

with the largest field-of-view (150 μm). When found, the flakes were first imaged with PEEM. Next we zoomed in, using LEEM, to a field-of-view of a few μm, and made a Bright Field image and an IV measurement.

One method to research CDWs are μLEED measurements. When there is a periodic density of charge in the crystal lattice, besides the zeroth and first order diffraction spots also intermediate spots will appear. The energy at which they appear and distance with the central spot can be used to find properties of the CDWs.

Noticeable is that when the gun spot had been pointed on a part of the flake, when afterwards looked with PEEM, a dark ellipse was seen on exactly this place, as shown in Figure 3.6. This means that something has changed while doing a measurement. The effect was more powerful when the energy of the electrons beam was higher. This probably was the effect of dirt that was now cleaned off the substrate and the flake by evaporation.

Chapter 4

Results & Discussion

4.1 Sample fabrication

In order to optimise the fabricated flakes, different methods of exfoliation are tested, as described in the previous chapter. The number of tapes used to exfoliate was varied, as well as the heating temperature and heating time during stamping. The hypothesis that more tapes used results in thinner flakes, turned out to only be partly true: when fewer tapes were used, most of the flakes that remain behind on the substrate were really thick, however there were always some flakes that were thin enough. Also, if more tapes were used the flakes became smaller. This is because every time exfoliated, the flakes get torn apart. And, because the force applied on the flakes is never precisely perpendicular, they also tear in the in-plane directions, resulting in smaller flakes. As can be seen in Figure 4.1a, b, c), where the number of tapes used is 2, 4 and 9 times respectively, the number and sizes of the flakes on the substrate differ considerably. The samples of (a) and (b) have more flakes than (c), while the flakes of (b) are the largest. Thus, an optimum is found in the use of four tapes, to get large and thin flakes.

The variation in temperature can be seen when Figure 4.1d) is compared with (b). The flakes on the sample of (d) are exfoliated four times and heated at 80 °C for 5 minutes while stamping. In optical photos, thin flakes are recognised by their darker, grey colour, while thick flakes appear white. It is noticeable that more flakes remain on the substrate when heating, however only very thick flakes. Few thin flakes remain behind. Also, the flakes are very wrinkled, indicating that they do not lie flat on the substrate and possibly water lies beneath the flakes. Another issue is that when heating, glue remains behind on the substrate. This is rather bothersome since there is now a high change that the flake that one would like to measure on is dirty and the substrate is overall very dirty. The glue can be washed off by sonicating in a bath of acetone just below the boiling point at 56°C. A major disadvantage is that when cleaning the samples after stamping, also a lot of flakes get washed of. And since one does not have any control on which flakes detach from the substrate, there is a chance that the flakes one wants to measure on get washed off.

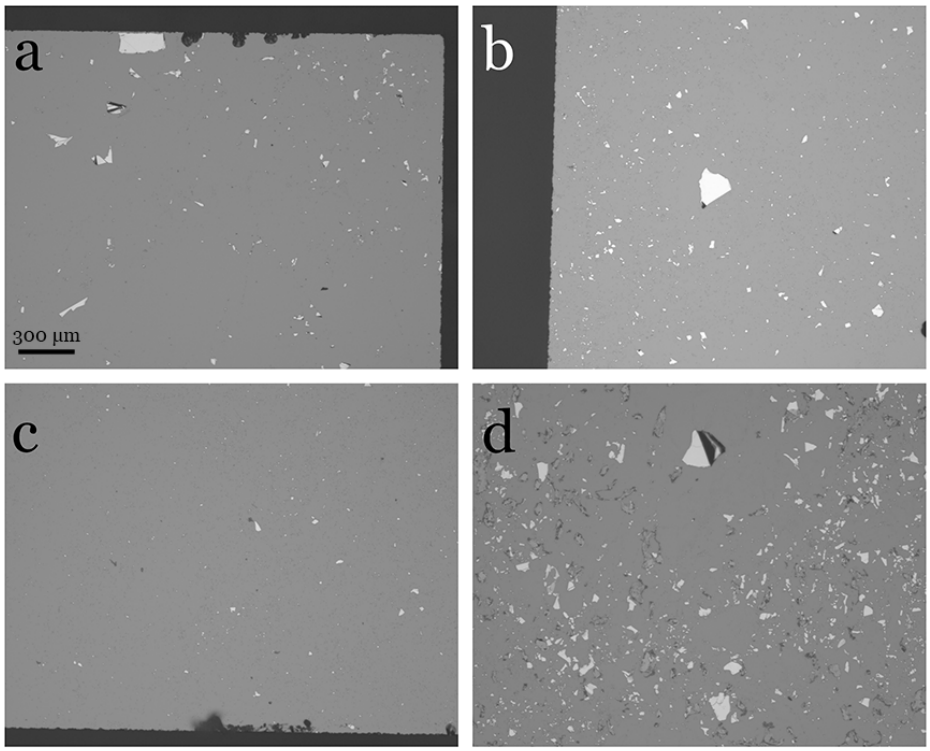

Figure 4.1: *Optical images of exfoliated TaS_2 on silicon dioxide.* (**a**, **b**, **c**) *Exfoliated 2, 4 and 9 times respectively.* (**d**) *Exfoliated 4 times and heated at 80 °C for 5 minutes while stamping.*

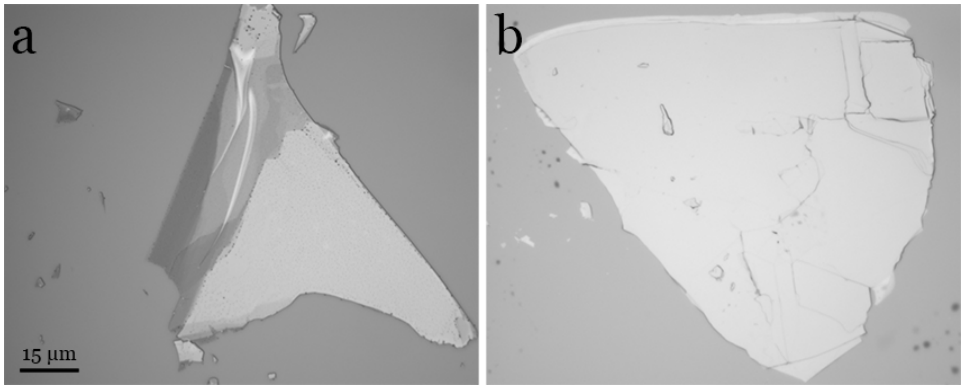

Figure 4.2: (**a**) *An optical image of exfoliated TaS_2 on silicon dioxide. A flake with varying thickness. The dark parts on the left are thin layers, of just a few layers thick.* (**b**) *An optical image of exfoliated TaS_2 on silicon. This flake is of a few hundred layers thick, because it is bright yellow in optical microscopy.*

After stamping, flakes were selected that were ideal for thickness identification and for LEEM measurements. For the former thin flakes with different thicknesses were needed. For the latter thick, large flakes were selected. An example of both can be seen in Figure 4.2.

4.2 Optical image analysis

The fabricated samples were photographed through an optical microscope, as described in Chapter 3. Figure 4.3 shows the contrast of every area compared with the substrate. This is done for every area, as shown in Figure 4.4, where a TaS_2 flake on (a) silicon dioxide, and (b) silicon is shown. The different colours on the photo represent the different thicknesses of the flake. Each area thus has a specific optical contrast with the substrate. The grey bars in Figure 4.3a) show the results for when black-and-white photos (taken with white light and with a blue and a red colour filter) are used, and the purple bars when a colour photo is used. There is a clear difference in the values of the contrasts. It is noticeable that for the colour photo the contrasts are in order from high to low. This is what one would expect, since, following the hypothesis, these are in order form thick to thin. This order of decreasing contrast is not present in the results for the black-and-white photos. These values firstly, lie closer together, and secondly, are in a "random" order.

According to our hypothesis that the colour corresponds to the thickness of the flake (from really thick to single layers the colours would go from yellow to blue to purple), the areas 1 to 4 are decreasing in thickness. The smallest difference in contrast with the substrate is between area 1 and 2, of just 0.062 ± 0.006. This value can be taken as a single layer difference. The thinnest part of the flake, area 4, has a contrast of 0.14 ± 0.01. With the assumption that the thickness depends linearly on the contrast, area 4 would be 2.3 the thickness of a single layer. Because there is always a discrete number of layers, this area is estimated to be two layers thick. In order to verify these results obtained from optical microscopy, AFM measurements of the same flakes were made, as is described in the next section.

This contrast determination is also done for flakes on silicon, of which the results of one flake are shown in Figure 4.3b). The areas correspond with the areas of the drawn line in Figure 4.4b). In the photo can be seen that, on this substrate, the flake has much less contrast differences, as described in Chapter 3. The values of the grey bars are obtained from a single black-and-white photo, taken with white light. Again, the values of the intensity of the contrast of each area compared with the substrate of the back-and-white photo differ greatly with the values of the colour photo. However, in this

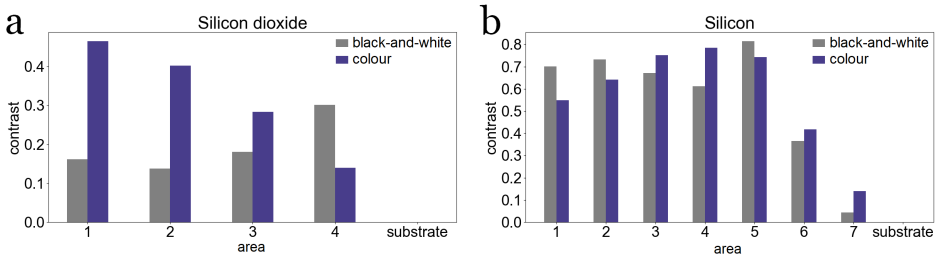

Figure 4.3: *The intensities of the contrast of the areas compared with the intensity of the substrate, plotted against the different areas. The grey bars are from a black-and-white photo, the purple bars from a colour photo.* (**a**) *Silicon dioxide substrate.* (**b**) *Silicon substrate.*

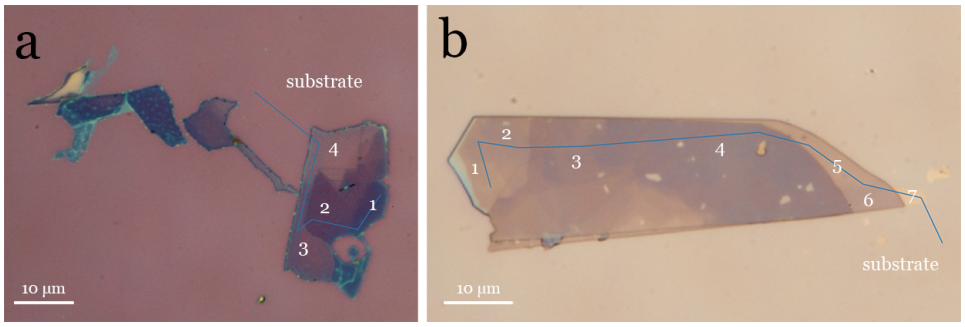

Figure 4.4: *Comparison of two TaS_2 flakes with varying thicknesses. Lines are drawn for for comparison of contrast as shown in Figure 4.3.* (**a**) *On a substrate of silicon dioxide,* (**b**) *On a substrate of silicon.*

case there is no decreasing order. This is because the thickness alternates (from area 1 to 4), but from area 4 to the substrate, the thickness decreases, and the values of the contrast of the colour photo decrease correspondingly.

4.2.1 Atomic Force Microscopy verification

The thickness of both flakes on silicon and on silicon dioxide in Figure 4.4 was measured with AFM. The results of the first can be seen in Figure 4.5. This part of the flake has areas of different thicknesses, showing different optical contrasts, as described in the previous section. The AFM image shows many higher spots on the flake. This is either dirt or oxidation and can thus be neglected. The boundaries of the areas seen in the optical photo can also be recognised in the AFM image. This means that there are height differences between these areas. The colour difference in (b) between these areas are small, but obvious. In the upper left corner is a height graph of the trace on the white line. There are two distinguishable levels, which correspond to the two areas (purple and pink in (a)). These areas differ only seven nm, or less than ten layers, with each other.

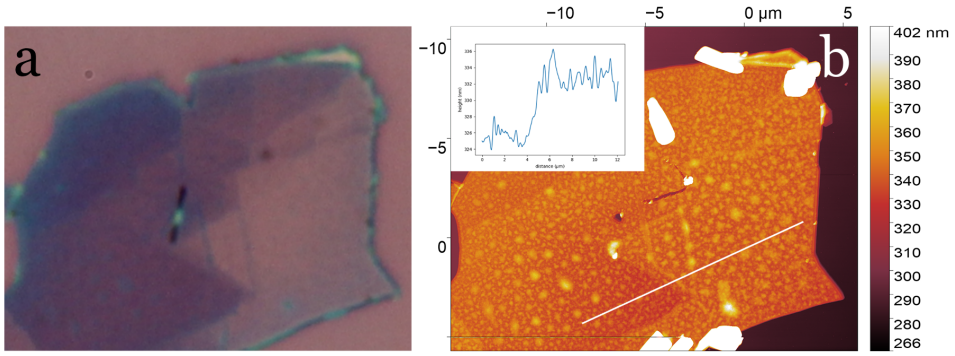

Figure 4.5: (**a**) *A part of the TaS_2 flake on silicon dioxide used for the optical image analysis.* (**b**) *AFM measurement of the same part of the flake. The different areas are noticeable in both images. The light circles are probably caused by oxidation. In the upper right corner is a height graph of the trace on the white line.*

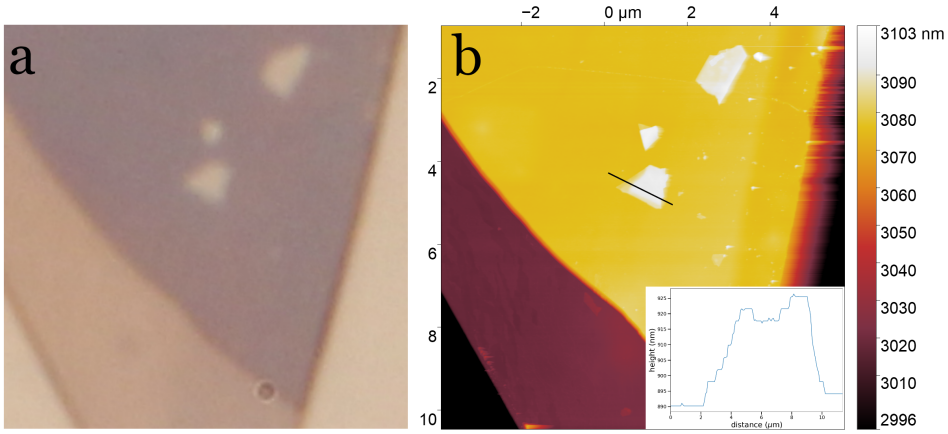

Figure 4.6: (**a**) *A part of the TaS_2 flake on silicon used for the optical image analysis.* (**b**) *AFM measurement of the same part of the flake. In the lower right corner is a height graph of the trace on the black line. Multiple steps of three nm can be seen.*

The flake on silicon in Figure 4.4b) is also measured with AFM, as can be seen in Figure 4.6. This left (thinner) part of the flake is approximately 810 layers thick. As described in the previous section, areas 4 to 6 are decreasing in thickness. In the lower right corner is a height graph of the trace on the black line, which is drawn over a small flake on top. in the graph there are clear steps of three nm visible. This means that the small flake has several edges of approximately ten layers difference.

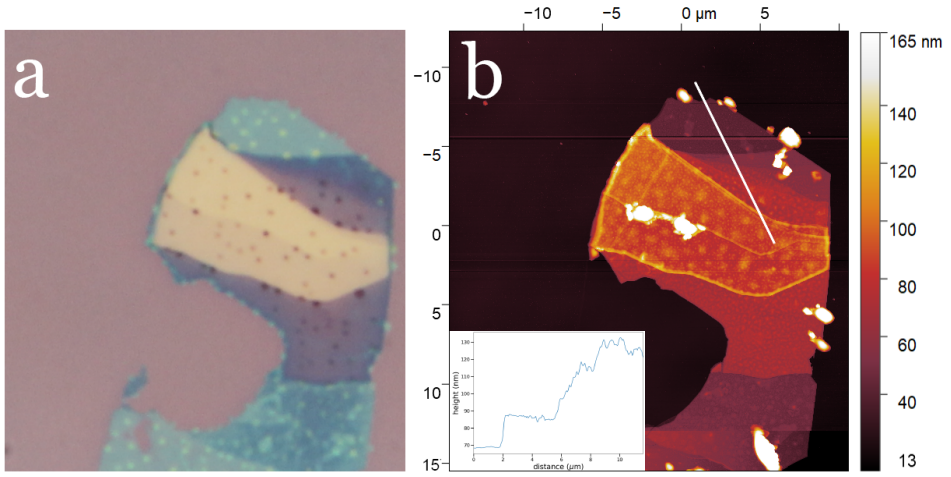

Figure 4.7: (**a**) *A TaS_2 flake on silicon dioxide. The flakes has various thicknesses, which result in the different colours.* (**b**) *An AFM measurement of the same flake. The separate areas are clearly visible as different heights. In the lower left corner is a height graph of the trace on the white line.*

Figure 4.7a) is an optical photo of a flake with various thicknesses. Following our hypothesis, the yellow area would be the thickest area, followed by the blue areas, and purple would be the thinnest areas. In the lower left corner of (b) is a height graph of the trace on the white line, which spans over several areas with different thicknesses. The yellow area is indeed very thick. However, according to the AFM measurement, the blue areas are actually thinner than the purple areas.

Beforehand the thinnest parts of the fabricated flakes were expected to be just a few layers thick. The results from the AFM measurements show that the thinnest fabricated flakes were still tens of layers thick. This does not mean that these flakes can not be used for research. The flakes are still very large and clean, and a lot thinner than bulk material, making them suitable for research. Besides large flat areas, there were also regions on flakes where the surface was not flat. Very thin layers lay on top of the surface and there were cavities of just a few layers deep. Thus, it is possible to create step edges of just a few layers. However, it would be more promising to perform research on flakes of just a few layers thick in order to study their two-dimensional effects. This could be done by fabricating thinner flakes.

It would however be optimal to be able to fabricate flakes of just a few layers thick, down to a single layer. The first thing that can be improved is the search for flakes. Because our hypothesis stated that the thinnest flakes were purple, these were most of the selected flakes. Now we know that the thinnest flakes are light blue, so these flakes should be selected.

4.3 Low Energy Electron Microscopy

Many parts of many flakes were measured with IV-LEEM, as described in Chapter 3. In Figure 4.8a) is a series of frames of an IV measurement shown. The closed body at the left side is a smaller flake lying on top, this can be neglected. At the first four frames, with lower energies, two domains with a different intensity can be distinguished. This is because they reflect a different intensity of electrons at these energies. However, at 32.0 and 34.7 eV a third and fourth domain emerge. This can also be seen in the IV plot in (b), where the intensity of the four domains is plotted against the energy of the electrons. From 28 eV onward, the four domains begin to differ. On this part of the flake all four domains differ greatly, although some domains only at higher energies. This might be due to the penetration depth, since electrons with a higher energy penetrate the flake deeper. Thus, when the energy rises, deeper structures could influence the intensity of the reflected electrons. These deeper structures also alter the band structure of the surface.

These structures were not expected to be seen, since the flakes were expected to be homogeneous and solely existing of the 1T-polytype. However, before measuring the sample was heated at 650 K, which is above the temperature of 550 K where the 1T-polytype gets unstable and transforms, resulting in a mix of the 2H-, 6R- and other polytypes. [4] This flake can be compared with other flakes. Whether they have the same different domains, absorbing and reflecting electrons with comparable intensities at the same energies.

In Figure 4.9a) is a second series from an IV measurement shown, of a different flake on the same sample. This is an edge of a flake (with the substrate at the lower right corner). On the flat part at the upper left corner of the flake, multiple domains can be seen. These domains have clear boundaries and are alternating in intensity. The fact that there are many different domains might be caused by the quality of the flake, or for example corrugation. If the material is corrugated, the same material can show different intensities. [28] From the straight diagonal line to the substrate, there are many step edges. Here, the flake gets thinner and thinner. This part of the flake has some remarkable regions. One region (area 5 in (b)) has a very high reflective intensity at 42.0 and 117.8 eV, while the rest of the flake has almost no intensity. This occurs at several other energies. It is also noticeable that the flake reflects electrons up to 150 eV, while MoS_2 only has an intensity up to 40 eV. [17] High energy electrons have a higher chance to scatter inelastically and are thus not imaged. This chance increases exponentially with the energy. [29] Due to these inelastically scattered electrons the intensity also falls off exponentially, as is the case with MoS_2. The same

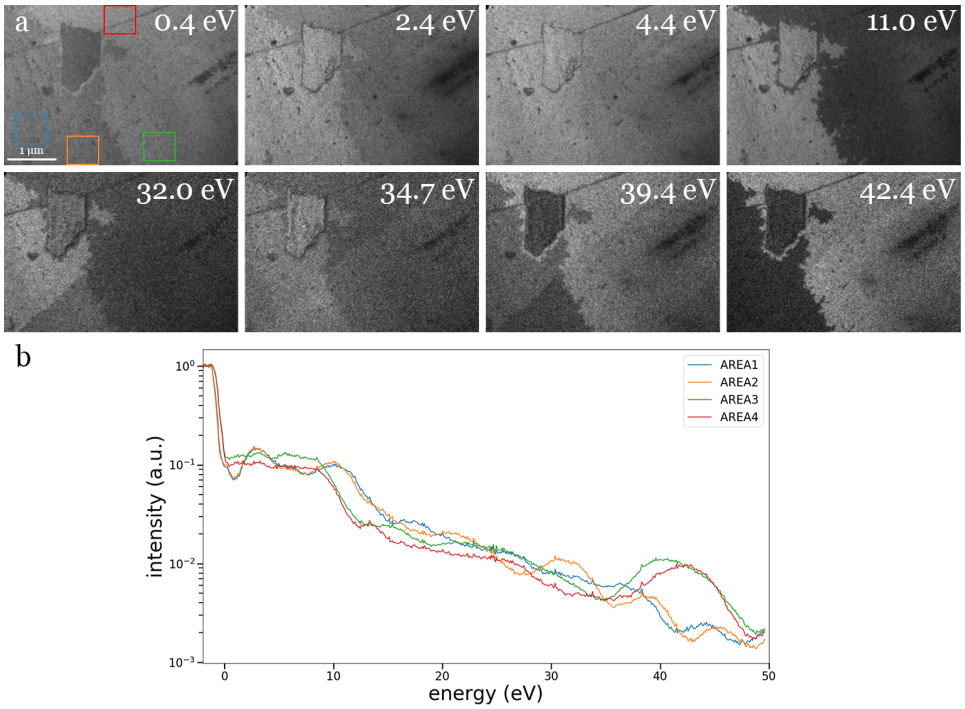

Figure 4.8: (**a**) *A series of frames taken from an IV measurement on a flake of TaS_2. This is the same area as phoographed through the optical microcope and measured with the AFM, as can be seen in Figure 4.6. The energies is denoted in the upper right corner in eV. Different areas are clearly distinguishable and alternate in intensity.* (**b**) *The corresponding IV plot with an energy from 0 to 50 eV.*

behaviour was expected for TaS_2. When the two IV plots in Figures 4.8b) and 4.9b) are compared, we see corresponding curves (area 1 and 2 on both flakes). These appear to be the same domains. There are however also totally non-corresponding curves. This means that there are many different domains possible on flakes of TaS_2.

Another interesting feature is the fact that the area indicated by the arrow in Figure 4.10 changed during the same measurement. The centre of this area turned abruptly from high intensity to low intensity at 64.4 eV. Directly after this, a wavefront moved over the rest of the area. This ends at 70.6 eV. Before the change this area was the same as the darker domain of area 3, however after the change this area is the same as the large domain of area 1. This can also be seen in Figure 4.9b), where the green line first follows the red line closely until $\pm$ 52 eV, and after 64.4 eV follows the blue line. If the contrast in the IV measurements is caused by different polytypes, than one polytype transformed into another here. During the measurement energy

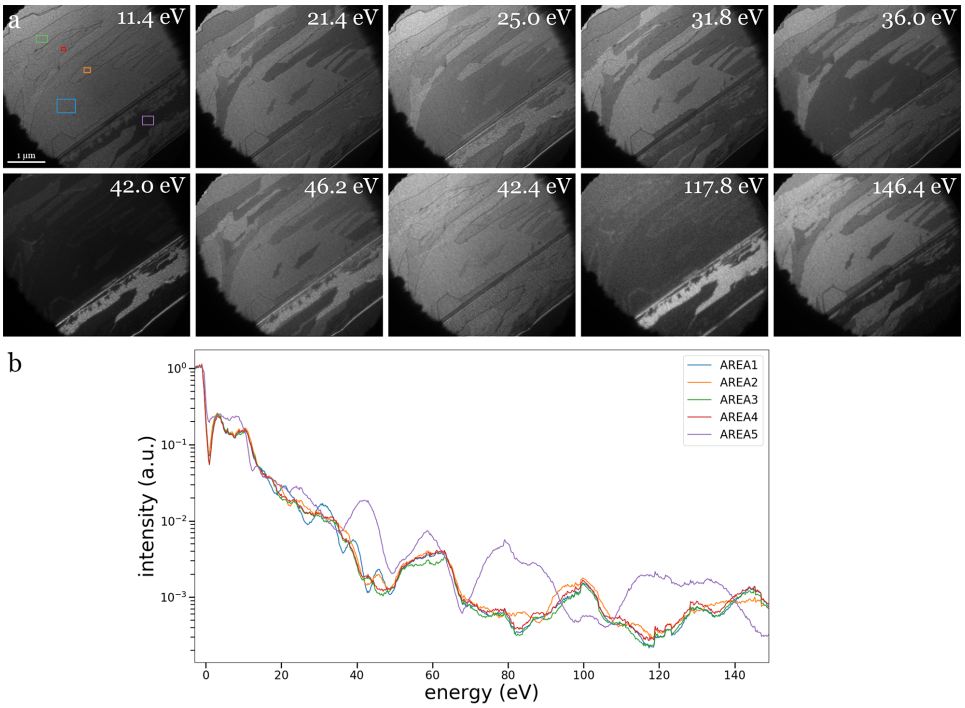

Figure 4.9: (**a**) *A second series of frames taken from an IV measurement on an edge of a flake of TaS_2. The energies is denoted in the upper right corner in eV. The substrate is visible in the lower right corner. Also here are different areas clearly distinguishable and alternate in intensity.* (**b**) *The corresponding IV plot with an energy from 0 to 150 eV.*

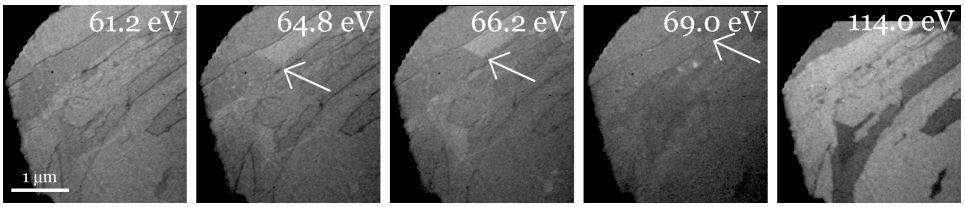

Figure 4.10: *A series of frames taken from the same IV measurement as Figure 4.9 (zoomed in on the upper left corner). The energies is denoted in the upper right corner in eV. The transformation of a domain is denoted with an arrow.*

is put into the flake, but because the electrons have very low energy, this is neglectable. However, also charge is put into the flake and the system gets doped with electrons. In this doped regime a different spacial structure could be energetically favourable and could thus trigger the transformation of one polytype into another.

A third measurement can be seen in 4.11. Here a flake with two thicknesses is shown, the upper and lower half of the view. The diagonal line coming

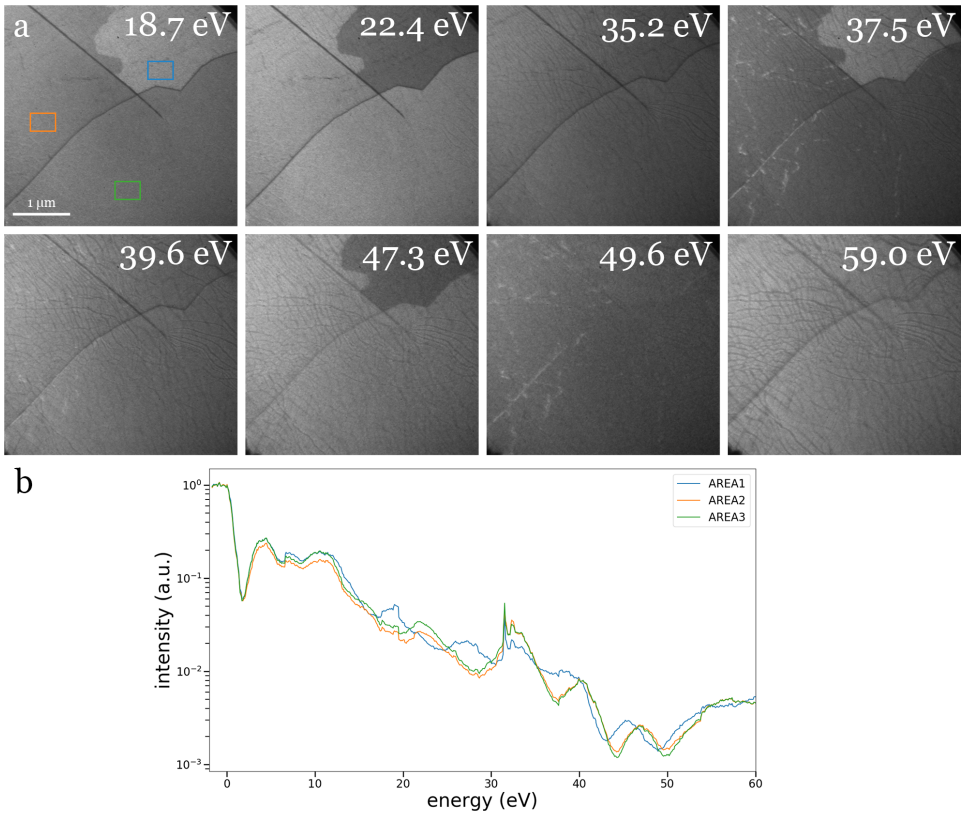

Figure 4.11: (**a**) *A third series of frames taken from an IV measurement on a flake of TaS_2. The energies is denoted in the upper right corner in eV. Different structures become visible at 35.2, 37.5, 49.6 and 59 eV.* (**b**) *The corresponding IV plot with an energy from 0 to 60 eV.*

in from the top is a fold. Three domains can clearly be distinguished. Noticeable are two different structures, of which the first are black lines. It looks like as if the flake is crackled and these lines appear for the first time at 35.2 eV. They disappear and reappear until it is extremely visible at 59 eV. The second structure can be seen at 37.5 and 49.6 eV. This consists of fewer and shorter bright lines. For both the dark and the bright domains the structures appear at the same locations for each energy.

Figure 4.12 shows an overview of a part of the flake, from edge to edge. Different domains can be seen on the whole flake. The measurement of Figure 4.9 was carried out on the large edge on the right side of this flake, just outside the overview. The measurement of Figure 4.11 on the red rectangle. These images were made at an energy of 14.8 eV.

Because the LEEM is very sensitive for the top layer of the material, dif-

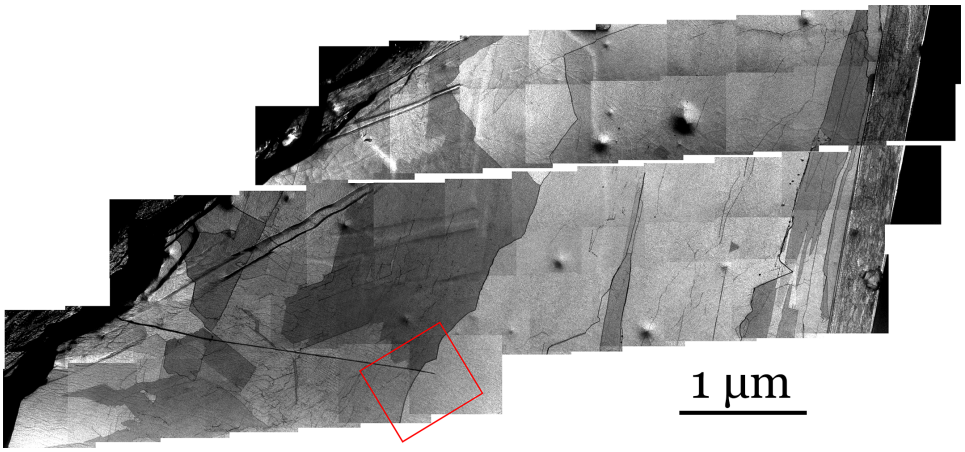

Figure 4.12: *Overview of a part of the flake with the large edge, taken at an energy of 14.8 eV. Different domains can be seen in perspective with the size of the flake. The red rectangle is the area measured in Figure 4.11.*

ferent terminations of unit cells, and thus different (variations of) polytypes, can possibly be distinguished. Below 550 K the 1T-polytype remains metastable, while above this temperature the 1T-polytype gets unstable and transforms, resulting in a mix of the 2H-, 6R-, and other polytypes. [4] The measurements done for this project were above this temperature. So these different polytypes could possibly be distinguished by measuring below this temperature.

Besides Bright Field measurements, also μLEED-measurements were performed. An aperture is inserted to limit the illuminated area. When in the diffraction plane is imaged the zeroth and first order diffraction spots are observed. Two adjacent first order spots correspond to the directions of the two reciprocal lattice vectors. First order spots appear when the incoming electrons have enough momentum to diffract to the adjacent atom. This momentum corresponds to the energy of the incoming electrons, since only the elastically scatters electrons are relevant. Thus when the energy of the incoming electrons is sufficient, constructive interference of electrons diffracted with the same angle result in the appearance of the first order diffraction spots. Figure 4.13a) shows the zeroth and first order diffraction spots at 35.0 eV. At 18.0 ± 0.1 eV the first order diffraction spots appear, as can be seen in Figure 4.13b, c, d). This energy can be used to calculate the lattice constant of the crystal, as described in Chapter 2.

When in diffraction space an IV measurement is taken on a localised area, the intensities of the zeroth and first order spots can be plotted. Two adjacent first order spots correspond to the directions of the two reciprocal

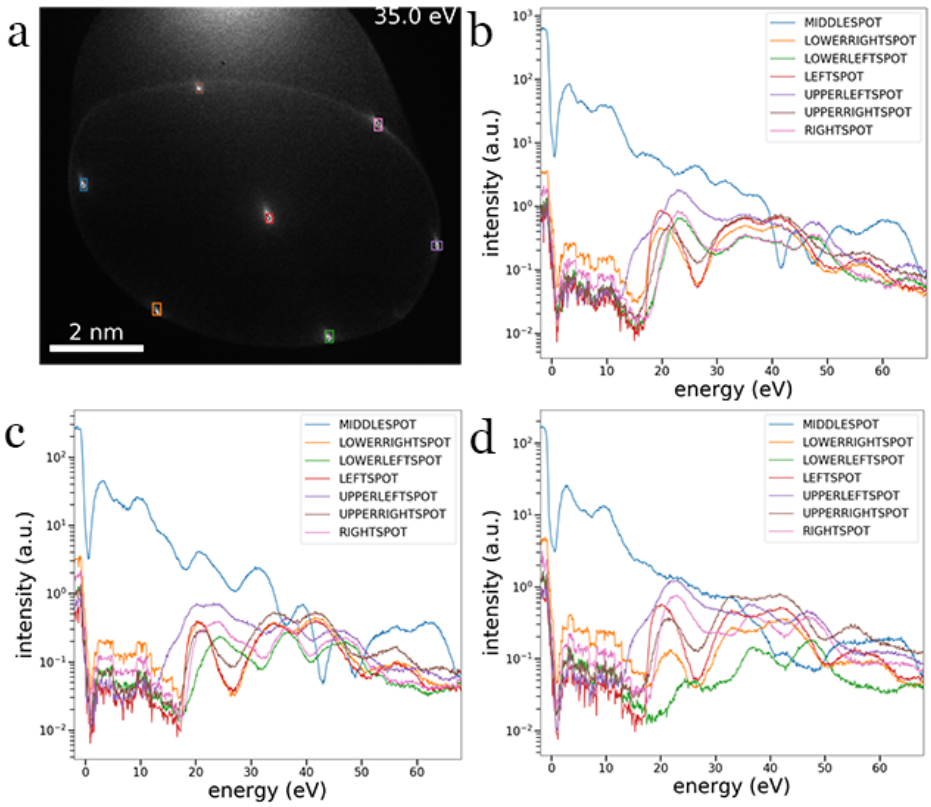

Figure 4.13: (**a**) *The zeroth and first order diffraction spots. Taken with a μLEED measurement with an energy of 35.0 eV.* (**b**, **c**, **d**) *IV plots of three different domains in the same flake as Figure 4.12. The first order diffraction spots come in at* 18.0 ± 0.1 *eV.*

lattice vectors. When the electrons have low energy, the angle of diffraction is insufficient to produce constructive interference with electrons diffracted on other atoms. This is expressed by Bragg's equation.

These lattice constants were calculated as early as in the seventies to be $a = b = 3.365$ Å, $c = 5.853$ Å for 1T-TaS_2 and $a = b = 3.316$ Å, $c = 12.070$ Å for 2H-TaS_2. [16] In the 2H-case the lattice constant is much greater than in the 1T-case because here the unit cell consists of two layers instead of one.

For all three μLEED measurements in Figure 4.13 the first order diffraction spots come in at 18.0 ± 0.1 eV. When we put this value into equation 2.6 we get $a = 3.34 \pm 0.01$ Å, which is only a 0.6% difference from the calculated $a = 3.316$ Å and 0.9% from $a = 3.365$ Å. The three areas can not be distinguished within the error margins and can thus either be the 1T- or the 2H-polytype. More accurate measurements should be done in order to be

able to distinguish the polytypes.

In μLEED measurements, no intermediate spots were observed, indicating that there were no CDWs present. This could be because the flakes were possibly not in the 1T-polytype. This is possible since the sample was heated above the transition temperature, possibly causing the 1T-polytype to completely transform into other polytypes. Another reason for the absence of CDWs could be that these flakes were more than a thousand layers thick.

4.3.1 Atomic Force Microscopy comparison

Figure 4.14a) is measured after the sample fabrication. This is the same area as the LEEM measurement in Figure 4.11. In between the fabrication and the measurement, the sample was stored in a vacuum and only two hours in the open air. Two large areas are present with an edge in between. The flake is thinner at the top than at the bottom of the image. The high diagonal line is a fold of the flake. One thing noticeable are the dark spots, both on the upper and on the lower half. These spots are thus lower than the surface. This can be caused by dirt on the sample, although this would result in spots higher than the surface, or maybe oxidation of the TaS_2. If the spots are caused by oxidation, than this has happened within the short time the sample was in the open air. In Figure 4.14b) the same area on the flake is measured again, this time after LEEM measurements. Now the dark spots are gone and the surface is smooth. This indicates that during the LEEM measurements the flake was cleaned, either with the heating or the fact that the sample was placed in a vacuum. Another cause can be the illumination of the gun spot, since we afterwards with PEEM saw elliptical imprints of the gun spot, as mentioned in Section 3.5.2. Another feature can be noticed when (b) and (c), which is made with LEEM measurements, are compared. The light structure seen in the lower corner in the second AFM image, that was not there before the LEEM measurements, is exactly the same domain boundary as seen in the LEEM image. This means that before the LEEM measurements there were no height differences of different domains, however during the measurements something has changed, resulting in a height difference on the edge of the domains.

There are however also a lot of structures, such as the light and dark lines, that can be seen with LEEM (compare with Figure 4.11a)), but not with AFM. This means that these structures do not vary in height and are thus hidden when measured with AFM.

The large edge of the flake in Figure 4.9a) is also measured with AFM (however rotated). In Figure 4.15a) is the edge shown, in (b) the flat part of the

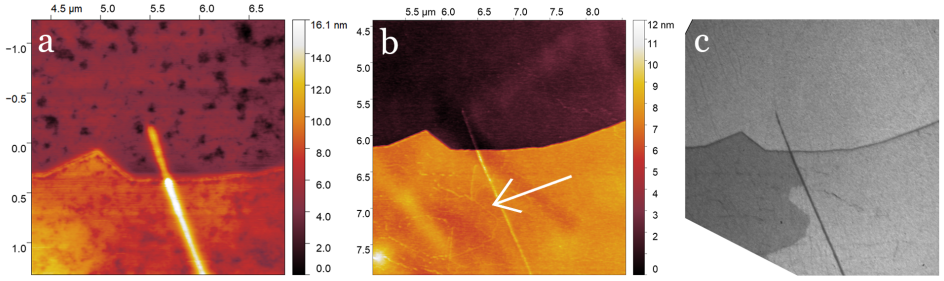

Figure 4.14: (**a**, **b**) *Two AFM measurements of the same part of a flake TaS_2. This is the same area as the LEEM measurement in Figure 4.11.* (**a**) *After sample fabrication.* (**b**) *After LEEM measurements. The dark spots have disappeared.* (**c**) *An image from the LEEM measurement on the same part of the flake. After LEEM measurements the same domain boundary can be seen with AFM, as denoted with an arrow.*

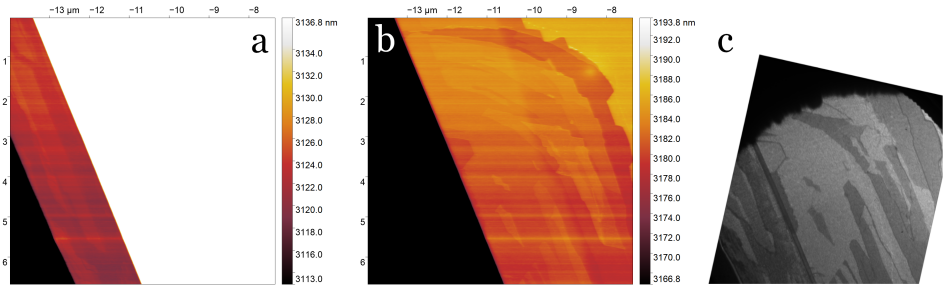

Figure 4.15: (**a**, **b**) *Two AFM measurements of the flake TaS_2 with the large edge. This is the same area as the LEEM measurement in Figure 4.9a).* (**c**) *An image from the LEEM measurement on the same part of the flake. The same domains can be seen with AFM and LEEM.*

flake and in (c) the LEEM measurement. The edge and the flat part were analysed separately, because they differ too much in height. By making two images instead of one, also the fine structures can be seen. The domains and structures seen in the LEEM measurements can also be seen in the AFM measurements. The height differences within the edge are rather small and the flake is even on this edge still very thick. Each domain seen on this large edge can be seen as a step edge. The flat part of the flake also exhibits a lot of structures.

Other structures that are visible in the LEEM results are the dark and bright lines that appeared at certain energies. These structures are not visible in the AFM results, so they do not come from height differences that the tip can resolve. What these structures are and what causes them is still unknown and may be interesting for future research into the material properties of TaS_2.

Chapter 5

Conclusion & Outlook

5.1 Sample fabrication

Before one can perform research on TaS_2, one has to fabricate samples. In order to get the cleanest substrate, one has to sonicate the sample in water, acetone and IPA at 45 °C, each for five to ten minutes. Then, the substrate should be blown dry with nitrogen and be ozone cleaned for at least fifteen minutes. Stamping should be performed as quickly as possible after the ozone cleaning.

As for the fabrication of samples, with exfoliation the usage of three or four tapes and no heating while stamping results almost every time in dozens of thin flakes large enough to perform LEEM measurements on. The samples should be properly stored. They should be in the open air for as short a time as possible and be stored in a desiccator in order to prevent oxidation.

5.2 Optical microscopy

Contradicting our hypothesis, the thinnest TaS_2 flakes observed on silicon dioxide are light blue. When the flakes get thicker, they go from dark blue, dark purple and pink to yellow. The thickest yellow flakes were measured to be a few hundred to more than a thousand of layers thick, as expected. In order to fabricate flakes of just single layers thick, the exfoliation process should thus be focused on and optimised for light blue flakes. Another possibility would be to grow thin flakes, similar what is done with the fabrication of bulk material.

With colour photos it can clearly be seen that the contrast of the TaS_2 flake with the substrate silicon dioxide rises as the flake gets thinner (Figure 4.4a) from area 4 to 1). This relation holds at least for the thinnest areas (in the pink, purple, blue regime). For TaS_2 flakes on silicon this relation is opposite: as the flake gets thinner, the contrast decreases (Figure 4.4b) from area 4 to 7). For future research the Python program LayerThicknessCalculator can thus be adjusted in order to calculate thickness ratios. It may even be possible to calibrate the program with AFM results, whereby not just the ratio of thicknesses can be found, but also the values of the thicknesses. The

calculated contrast values of the colour photos were more useful and made more sense than those of the black-and-white photos. I therefore strongly advise the purchase of a colour camera to install on the microscope, which can communicate with the software.

5.3 Low Energy Electron Microscopy

The first thing that stands out from the LEEM results is the reflection of electrons pursuing until an energy of 150 eV. This reveals that the unoccupied band structure of TaS_2 is richer than expected. This band structure can be researched using Angle-Resolved Reflected-Electron Spectroscopy (ARRES) measurements.

Noticeable are the different domains on the flakes, as seen in the LEEM results. When IV curves of these areas are compared, we can conclude that there are at least six types of domains. The flake existing of different polytypes could be the cause for the observed contrasts. To confirm whether the observed domains are caused by different polytypes, IV measurements should be done at temperatures where the 1T-polytype is stable.

When these areas are compared with the AFM results, the boundaries of the domains can be seen. There is thus a small raised edge where these domains meet. This could be because by the possibility that when two different crystalline structures meet, there is never a perfect transition, which could lead to these raised edges. Hence, this suggests that these domains are caused by different polytypes.

As for CDWs, further research should be done on TaS_2 flakes. IV measurements can be performed at a temperature below 550 K, where the 1T-polytype is stable. Also, flakes of just a few layers thick should be measured.

In conclusion, the optical and electronic properties of TaS_2 are far more complex than expected. There are still many questions regarding its band structure and other properties and more research has to be done on this remarkable material.

Bibliography

[1] P. R. Wallace, *The band theory of graphite*, Physical Review **71**, 622 (1947).

[2] K. Novoselov and A. Geim, *Electric Field Effect in Atomically Thin Carbon Films*, Science **306**, 666 (2004).

[3] H. Li, G. Lu, Y. Wang, Z. Yin, C. Cong, Q. He, L. Wang, F. Ding, T. Yu, and H. Zhang, *Mechanical exfoliation and characterization of single- and few-layer nanosheets of WSe2, TaS2, and TaSe2*, Small **9**, 1974 (2013).

[4] J. A. Wilson, F. J. Di Salvo, and S. Mahajan, *Charge-density waves and superlattices in the metallic layered transition metal dichalcogenides*, Adv. Phys. **32**, 1171 (1974).

[5] A. W. Tsen, R. Hovden, D. Wang, Y. D. Kim, J. Okamoto, K. A. Spoth, Y. Liu, W. Lu, Y. Sun, J. C. Hone, L. F. Kourkoutis, P. Kim, and A. N. Pasupathy, *Structure and control of charge density waves in two-dimensional 1T-TaS2*, Proceedings of the National Academy of Sciences **112**, 15054 (2015).

[6] R. Hovden, A. W. Tsen, P. Liu, B. H. Savitzky, I. El Baggari, Y. Liu, W. Lu, Y. Sun, P. Kim, A. N. Pasupathy, and L. F. Kourkoutis, *Atomic lattice disorder in charge-density-wave phases of exfoliated dichalcogenides (1T-TaS2)*, Proceedings of the National Academy of Sciences **113**, 11420 (2016).

[7] Á. Pásztor, A. Scarfato, and C. Renner, *Mechanical in situ exfoliation of van der Waals materials*, Review of Scientific Instruments **88**, 076104 (2017).

[8] H. Li, J. Wu, Z. Yin, and H. Zhang, *Preparation and applications of mechanically exfoliated single-layer and multilayer MoS2 and WSe2 nanosheets*, Accounts of Chemical Research **47**, 1067 (2014).

[9] Z. Zeng, Z. Yin, X. Huang, H. Li, Q. He, G. Lu, and F. Boey, *Single-Layer Semiconducting Nanosheets : High-Yield Preparation and Device Fabrication*, Angewandte Chemie - International Edition **50**, 11093 (2011).

[10] I. Song, C. Park, and H. C. Choi, *Synthesis and properties of molybdenum disulphide: from bulk to atomic layers*, RSC Adv. **5**, 7495 (2015).

[11] Y. Huang, E. Sutter, N. N. Shi, J. Zheng, T. Yang, D. Englund, H. J. Gao, and P. Sutter, *Reliable Exfoliation of Large-Area High-Quality Flakes of Graphene and Other Two-Dimensional Materials*, ACS Nano **9**, 10612 (2015).

[12] J. N. Coleman, *Two-Dimensional Nanosheets Produced by Liquid Exfoliation of Layered Materials Two-dimensional nano-sheets produced by liquid exfoliation of layered materials*, Science **331**, 568 (2011).

[13] C. J. Shearer, A. D. Slattery, A. J. Stapleton, J. G. Shapter, and C. T. Gibson, *Accurate thickness measurement of graphene*, Nanotechnology **27**, 1 (2016).

[14] L. B. P. Nemes-Incze, Z. Osváth, K. Kamarás, *Anomalies in thickness measurements of graphene and FLG crystals by tapping mode AFM*, Carbon **46**, 1435 (2008).

[15] M. Chhowalla, H. S. Shin, G. Eda, L. J. Li, K. P. Loh, and H. Zhang, *The chemistry of two-dimensional layered transition metal dichalcogenide nanosheets*, Nature Chemistry **5**, 263 (2013).

[16] L. F. Mattheiss, *Band Structures of Transition Metal Dichalcogenide Layer Compounds*, Phys. Rev. B **8**, 3719 (1973).

[17] T. A. de Jong, *Stacking domains in bilayer Van der Waals materials*, Master's thesis, 2017.

[18] I. Jung, M. Pelton, R. Piner, D. A. Dikin, S. Stankovich, S. Watcharotone, M. Hausner, and R. S. Ruoff, *Simple approach for high-contrast optical imaging and characterization of graphene-based sheets*, Nano Letters **7**, 3569 (2007).

[19] J. Kröger, *Electron-phonon coupling at metal surfaces*, Reports on Progress in Physics **69**, 899 (2006).

[20] *HQ Graphene. Available from: http://hqgraphene.com*.

[21] H. Li, J. Wu, X. Huang, G. Lu, J. Yang, X. Lu, Q. Xiong, and H. Zhang, *Rapid and reliable thickness identification of two-dimensional nanosheets using optical microscopy*, ACS Nano **7**, 10344 (2013).

[22] T. Uwanno, Y. Hattori, T. Taniguchi, K. Watanabe, and K. Nagashio, *Fully dry PMMA transfer of graphene on h-BN using a heating/ cooling system*, 2D Materials **2**, 41002 (2015).

[23] G. Binnig and C. F. Quate, *Atomic Force Microscope*, Physical Review Letters **56**, 930 (1986).

[24] W. Walczyk, P. M. Schön, and H. Schönherr, *The effect of PeakForce tapping mode AFM imaging on the apparent shape of surface nanobubbles*, Journal of Physics Condensed Matter **25** (2013).

[25] *Gwyddion. Available from http://gwyddion.net*.

[26] R. M. Tromp, J. B. Hannon, a. W. Ellis, W. Wan, A. Berghaus, and O. Schaff, *A new aberration-corrected, energy-filtered LEEM/PEEM instrument I. Principles and design*, Ultramicroscopy **110**, 1 (2010).

[27] R. M. Tromp, J. B. Hannon, W. Wan, A. Berghaus, and O. Schaff, *A new aberration-corrected, energy-filtered LEEM/PEEM instrument II. Operation and results*, Ultramicroscopy **127**, 25 (2013).

[28] A. Locatelli, K. R. Knox, D. Cvetko, O. Mentes, M. A. Nin, S. Wang, M. B. Yilmaz, P. Kim, R. M. Osgood, and A. M. , *Corrugation in Exfoliated Graphene : An Electron Microscopy and Diffraction Study*, ACS Nano **4**, 4879 (2010).

[29] D. Geelen, *eV-TEM: Transmission Electron Microscopy with few-eV electrons*, PhD thesis, 2018.

Acknowledgements

Firstly I want to thank Tobias de Jong and Sense Jan van der Molen for their supervision throughout my bachelor project and for creating a pleasant and open working ambiance. I want to thank Jan van Ruitenbeek for coreading my thesis and attending my final presentation.

A big thanks to Dennis Uitenbroek for all the useful, but hilarious discussions and wanting to share an office with me. Finally thanks to Lennard Kwakernaak for all the discussions and all his Python knowledge.